



## **DATforDCEMRI: An R Package for Deconvolution Analysis and Visualization of DCE-MRI Data**

**Gregory Z. Ferl**  
Genentech

---

### **Abstract**

Numerical deconvolution is a powerful mathematical operation that can be used to extract the impulse response function of a linear, time-invariant system. We have found this method to be useful for preliminary analysis of dynamic contrast enhanced magnetic resonance imaging (DCE-MRI) data, capable of quickly producing voxel-wise parametric maps describing the heterogeneity of contrast agent kinetics over the entire field of view, typically comprising tens of thousands of voxels. The statistical programming language R is well suited for this type of analysis and when combined with  $\text{\LaTeX}$ , via *Sweave*, allows one to perform all calculations and generate a report with a single script. The purpose of this manuscript is to describe the R package **DATforDCEMRI**, a Deconvolution Analysis Tool for DCE-MRI contrast agent concentration vs. time data, which allows the user to perform kinetic deconvolution analysis and visualize/explore the resulting voxel-wise parametric maps and associated data.

*Keywords:* DCE-MRI, clinical, malignant, tumor, deconvolution, pharmacokinetics, pharmacodynamics, R.

---

## **1. Introduction**

Dynamic contrast enhanced magnetic resonance imaging (DCE-MRI) is commonly used to assess changes in vascular structure subsequent to dosing with an anti-angiogenic agent such as bevacizumab. The measured signal intensity within the tissue of interest is altered by leakage into extravascular, extracellular tissue space (EES) of a low molecular weight contrast agent that is injected subsequent to start of data acquisition. Vascular permeability, surface area, tissue perfusion rate and EES volume will impact the pharmacokinetic profile of the contrast agent within tissue, which can be described by estimating physiologically relevant parameter values via compartmental modeling. Ideally, a patient will be scanned twice prior to treatment to establish inter-visit variability, with additional scans acquired hours to days after the first

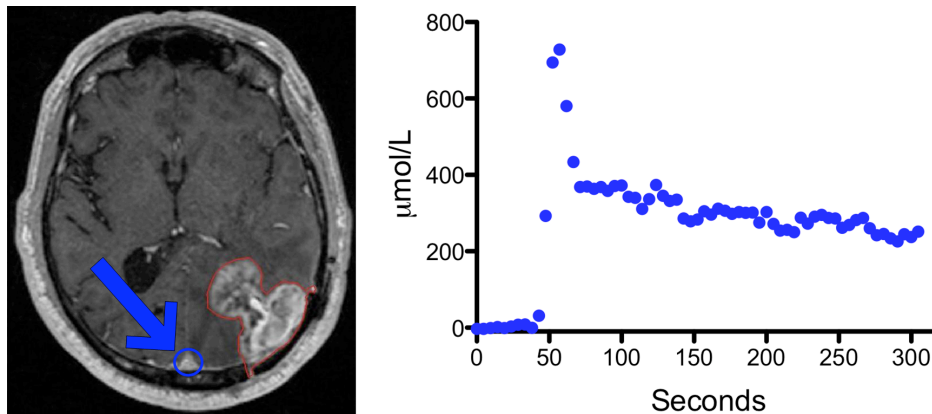


Figure 1: Post-contrast static  $T_1$  weighted image (axial slice) showing the *approximate* location of the superior sagittal sinus (blue circle), used to estimate the AIF shown in the right-hand panel. The region of interest corresponding to contrast enhanced tumor is outlined in red (left-hand panel).

dose. Estimated model parameters are compared across scans to assess the apparent impact of drug on tissue vascular structure. The interested reader is directed to Padhani (2002), Choyke *et al.* (2003), O’Connor *et al.* (2007) and Tofts *et al.* (1999) for details.

Here, we extend our previously described numerical deconvolution method for kinetic analysis of DCE-MRI data (Ferl *et al.* 2010) with a focus on the utility of the statistical programming language R (R Development Core Team 2011) as a tool for performing computational and data visualization tasks. Briefly, Ferl *et al.* (2010) describes an R script that imports whole tumor and vascular region of interest (ROI) contrast agent concentration data, subtracts a nominal blood fraction from the tumor data, removes all pre-peak vascular data and associated tumor data, smooths the vascular and tumor curves using the **lofit** package (Loader 1999, 2010), performs the numerical deconvolution operation on the smoothed data and calculates noncompartmental parameters associated with the resulting impulse response function (IRF). Noncompartmental parameters, namely area under the IRF curve from  $t = 0$  to  $t = T_f$  ( $AUC_{T_f}$ ) and the ratio of  $AUC_{T_f}$  to the mean residence time of the IRF between  $t = 0$  and  $t = T_f$  ( $MRT_{T_f}$ ), are compared to estimated model parameters ( $K^{\text{trans}}$  and  $v_e$ , respectively) and shown to be comparable, particularly when assessing treatment effect by comparing percent change of parameters associated with a post-treatment scan relative to pre-treatment baseline scans. The Tofts version of the Kety model (Kety 1951) is described in Tofts and Kermode (1991).

We’ve significantly extended our deconvolution script to perform voxel-wise (as opposed to whole ROI) analysis of all tissue within the MRI field of view (FOV) and developed an interactive Advanced Voxel Diagnosis Tool (AVDT) that can be used to explore parametric maps generated by the deconvolution analysis. Voxel-wise analysis of DCE-MRI data gives insight into heterogeneity of tumor vascular structure and drug response that is not apparent from whole-tumor analysis. All R code required to perform these tasks is accessible via the package **DATforDCEMRI** (Ferl 2011), available from the Comprehensive R Archive Network (CRAN) at <http://CRAN.R-project.org/package=DATforDCEMRI>.

Due to the iterative nature of parameter estimation, computational time is significant when

performing voxel-wise parameter estimation using a compartmental model. Numerical deconvolution is much faster when compared to other parametric methods and thus is appealing as a tool for initial quantitative analysis of DCE-MRI data. Potential ROIs, treatment effects and initial parameter values for subsequent analysis, e.g., compartmental modeling (Whitcher and Schmid 2011a,b), can all be gleaned using our approach; a collection of R packages for medical image analysis may be found on CRAN Task Views (Zeileis 2005) under the category “Medical Imaging” (Whitcher 2010).

`Sweave` (Leisch 2002), a function within the `utils` package (R Development Core Team 2011) that is part of every R installation, was utilized to prepare this manuscript in a literate programming environment (Knuth 1984). The code shown here has not been cut and pasted into the document; typesetting and execution of the R code occurred in the same run so that we can be sure that the code appearing here is exactly that which produced the associated figures.

## 2. Materials and methods

### 2.1. Data files

An arterial input function (AIF), in this case blood concentration of contrast agent in the brain, is shown in the right panel of Figure 1. In addition to an  $n_f \times 1$  time vector, the corresponding data file contains an  $n_f \times 1$  AIF vector representing median contrast agent concentrations within an ROI drawn around the superior sagittal sinus (Figure 1, left panel) for each time point listed in a separate time vector.

Two additional data sets must be specified in order to perform voxel-wise analysis; (1) Contrast agent concentrations stored in an  $n_x \times n_y \times n_z \times n_f$  matrix where  $n_x \times n_y$  are the dimensions of the FOV,  $n_z$  is the number of slices and  $n_f$  is the number of data frames / time points, and (2) an ROI mask stored as an  $n_x \times n_y \times n_z$  matrix of 1’s and 0’s, where 1 indicates a voxel to be analyzed. These and other symbols used here are listed in Table 1.

Data to be analyzed by `DATforDCEMRI` can be stored in any file format, as long as it can be read into R. For example, the package `R.matlab` contains the `readMat` function, which may be used to import uncompressed MATLAB files into R. The function `read.csv`, a specific form of the more general `read.table` function from the `R.utils` package (Bengtsson 2011), can be used to import data that has been saved in the csv format. Results of the deconvolution analysis are saved in the `RData` file format by default.

The function `DAT.checkData`, contained within the `DATforDCEMRI` package, is used to create a data file that can be run by the `DAT` function (Table 2). The AIF, time vector, ROI mask and contrast agent concentration array serve as arguments to this function, as described in the package documentation and the sample session within this paper.

### 2.2. Data smoothing

The deconvolution operation is highly sensitive to noisy data, motivating us to implement the adaptive smoother within the `locfit` (Loader 2010) package. The R code smooths each voxel-wise vector of measured contrast agent concentration-time data ( $\vec{C}_f$ ) and the measured vector of arterial input function ( $\vec{AIF}_f$ ) values using empirically derived computational settings that

---

$u(t)$	Generic representation of a system input.
$y(t)$	Generic representation of an observed system output.
$h(t)$	Generic representation of the Impulse Response Function ( <i>IRF</i> ).
$C_t(t)$	Contrast agent concentration in tumor.
$\text{AIF}(t)$	Arterial Input Function; concentration of contrast agent in blood.
$\text{IRF}(t)$	Impulse Response Function; tissue response to a unit strength input, $\delta(t)$ .
$\vec{C}_f$	$n_f \times 1$ vector of measured contrast agent concentrations in tissue.
$\vec{\text{AIF}}_f$	$n_f \times 1$ vector of measured contrast agent concentrations in blood.
$\vec{C}_s$	$n_s \times 1$ vector of smoothed $\vec{C}$ values.
$\vec{\text{AIF}}_s$	$n_s \times 1$ vector of smoothed $\vec{\text{AIF}}$ values.
$\mathbf{AIF}_s$	$n_s \times n_s$ convolution matrix composed of $\vec{\text{AIF}}_s$ values.
$\vec{h}_s$	$n_s \times 1$ vector of IRF values.
$\text{AUC}_{T_f}$	Area under the curve of $\vec{\text{IRF}}$ from $t = 0$ to $t = T_f$ .
$\text{MRT}_{T_f}$	Mean residence time of $\vec{\text{IRF}}$ from $t = 0$ to $t = T_f$ .
$\text{AUC}_\infty$	Area under the curve of $\vec{\text{IRF}}$ ( $t = 0$ to $t = \infty$ ).
$\text{MRT}_\infty$	Mean residence time of $\vec{\text{IRF}}$ ( $t = 0$ to $t = \infty$ ).
$z$	Slice number.
$n_s$	Length of $\vec{C}$ and $\vec{\text{AIF}}$ smoothed vectors ( <b>locfit</b> output).
$n_f$	Number of frames in the DCE-MRI data.
$n_x$	Number of voxels within the field of view (x-axis).
$n_y$	Number of voxels within the field of view (y-axis).
$n_z$	Number of voxels within the field of view (z-axis/number of slices).
$T_f$	Duration of DCE-MRI scan.
$K^{\text{trans}}$	Plasma/tissue contrast agent exchange rate.
$v_e$	Fractional tissue volume accessible to contrast agent.
$v_b$	Fractional whole blood volume in tissue.

---

Table 1: Definitions of symbols used in this manuscript.

retain the sharp peak of the blood curve while down-weighting apparent outlier data points in the plasma and tumor curves. The behavior of the smoothing curve may be altered by increasing or decreasing the components of the smoothing parameter, **alpha**; i.e., an overly smoothed curve may not capture the sharp peak of  $\vec{\text{AIF}}_f$ , while undersmoothing may yield a noisy curve. Prior to smoothing, the original  $\vec{C}_f$  and  $\vec{\text{AIF}}_f$  vectors are transformed by removing all pre-peak  $\vec{\text{AIF}}_f$  (and corresponding  $\vec{C}_f$ ) data and shifting the  $\vec{C}_f$  curve by one



Figure 2: Schematic representation of a generic convolution operation, where  $u(t)$  represents the system input,  $y(t)$  represents the system output and  $h(t)$  is the IRF, depicted in the right-hand panel as the observed system output in response to a unit strength impulse,  $\delta(t)$ .

Name	Description
<code>DAT</code>	Kinetic data analysis and visualization.
<code>DAT.checkData</code>	Data file generation and validation.
<code>DAT.simData</code>	A simulated DCE-MRI data set.

Table 2: Contents of the **DATforDCEMRI** package.

frame to partially compensate for venous-arterial time lag (Ferl *et al.* 2010). The smoothing functions yield the smoothed  $\vec{C}_f$  and  $\vec{\text{AIF}}_f$  vectors,  $\vec{C}_s$  and  $\vec{\text{AIF}}_s$ , which serve as arguments for the deconvolution function.

### 2.3. Numerical deconvolution

Numerical deconvolution is discussed by Rescigno and Segre (1966) and Evans (1954), with applications to DCE-MRI covered by Ferl *et al.* (2010) and Fan and Karczmar (2009). Additionally, a semiparametric approach to DCE-MRI kinetic analysis using Bayesian P-splines is described in Schmid *et al.* (2009). Briefly, the *convolution* operation relates input and output for a linear, time-invariant system via the IRF as shown schematically in Figure 2. Given a system input  $u(t)$  and the function  $h(t)$ , the output  $y(t)$  can be computed by convolution of  $u(t)$  and  $h(t)$ . In the case of DCE-MRI kinetic analysis, these variables are defined as:

$$u(t) = \text{AIF}(t), \tag{1}$$

$$h(t) = \text{IRF}(t), \tag{2}$$

$$y(t) = C_t(t) \tag{3}$$

where  $C_t(t)$  is the observed contrast agent concentration in tumor (or any other tissue of interest) and  $\text{AIF}(t)$  is the arterial input function, so that

$$C_t(t) = \text{AIF}(t) \otimes \text{IRF}(t) = \int_{-\infty}^{\infty} \text{AIF}(\tau) \text{IRF}(t - \tau) d\tau, \tag{4}$$

where  $\otimes$  is the convolution operator. Given discretized values of  $\text{AIF}(t)$  and  $h(t)$ , the convolution operation is performed via vector matrix multiplication:

$$\vec{C}_s = \mathbf{AIF}_s \vec{\text{IRF}}, \tag{5}$$

where  $\vec{C}_s$  and  $\vec{\text{IRF}}$  are  $1 \times n_s$  vectors and  $\mathbf{AIF}_s$  is an  $n_s \times n_s$  matrix (Ferl *et al.* 2010).

In the case of DCE-MRI analysis, we have estimates of  $\vec{C}_s$  and  $\mathbf{AIF}_s$  and can retrieve the IRF by solving for  $\vec{\text{IRF}}$ .

The basic numerical deconvolution function written for **DATforDCEMRI** (Ferl *et al.* 2010) operates on smoothed  $\vec{C}_f$  and  $\vec{\text{AIF}}_f$  vectors of equal length ( $\vec{C}_s$  and  $\vec{\text{AIF}}_s$ ) and returns the impulse response function ( $\vec{\text{IRF}}_s$ ) and all associated **lofit** objects.

## 2.4. The Kety model

Briefly, the Tofts version of the Kety model (Kety 1951; Tofts and Kermode 1991) may be written as

$$\frac{dC_t(t)}{dt} = \text{AIF} \cdot K^{\text{trans}} - C_t(t)k_{\text{ep}}, \quad (6)$$

where the corresponding IRF is

$$h(t) = K^{\text{trans}} e^{-k_{\text{ep}}t}. \quad (7)$$

The parameter  $K^{\text{trans}}$  represents fractional rate of contrast agent flux between plasma and interstitial space and is physiologically interpreted as an amalgam of tissue perfusion rate, capillary surface area and capillary permeability. The parameter  $k_{\text{ep}} = K^{\text{trans}}/v_e$ , where  $v_e$  represents the fractional volume of the interstitial space that is accessible to contrast agent (EES). A detailed discussion of model notation and physiological interpretation can be found in Tofts *et al.* (1999).

The extended Tofts version of the Kety model (Tofts 1997) explicitly considers the contribution of intravascular contrast agent to total tissue signal by adding  $v_b$  to the measurement model, written as

$$C(t) = C_t(t) + v_b \text{AIF}, \quad (8)$$

where the parameter  $v_b$  represents fractional whole blood volume in the tissue of interest.

The Tofts version of the Kety model is fitted to voxel-wise data using an in-house kinetic analysis tool programmed in R (not included in **DATforDCEMRI**). Briefly, optimal parameter values are calculated by minimizing a maximum likelihood objective functional of the form

$$J(p) = \frac{1}{n_f} \sum_{i=1}^{n_f} \left[ \frac{(s(\hat{p}, t_i) - d_i)^2}{\text{SD}^2} + \ln(\text{SD}^2) \right], \quad (9)$$

using the *Nelder-Mead* optimization method implemented by the `optim()` function. The number of data points within each contrast agent curve is indicated by  $n_f$ ,  $s(\hat{p}, t_i)$  is the simulated contrast agent concentration at time  $i$  and parameter vector  $\hat{p}$  within the parameter space under consideration and  $d_i$  is the measured contrast agent concentration at time  $i$ . The analytical solution of Equation 6 is used during the fitting process to reduce computational time and is achieved by describing the AIF with a two compartment model and solving the resulting system of three ODEs for  $C_t(t)$ . Data is uniformly weighted by setting the standard deviation (SD) to unity for all data points.

## 2.5. Noncompartmental analysis

The truncated area under the curve ( $\text{AUC}_{T_f}$ ) and mean residence time ( $\text{MRT}_{T_f}$ ) of  $\vec{\text{IRF}}$  vectors are calculated by the `DAT` function using the trapezoidal rule.  $\text{MRT}_{T_f}$  is equal to the area under the first moment curve ( $\text{AUMC}_{T_f}$ ) divided by  $\text{AUC}_{T_f}$ , as described in Ferl *et al.* (2010).  $\text{AUC}_{T_f}$ ,  $\text{MRT}_{T_f}$  and  $\text{AUC}_{T_f}/\text{MRT}_{T_f}$  are returned by `DAT`.

Object	Description
<code>vectorTimes</code>	Original $1 \times \text{nt}$ vector of data acquisition time points.
<code>maskROI</code>	Original $\text{nx} \times \text{ny}$ region of interest mask.
<code>mapCC</code>	Original $\text{nx} \times \text{ny} \times \text{nt}$ matrix of contrast agent concentrations.
<code>vectorAIF</code>	Original $1 \times \text{nt}$ arterial input function vector.
<code>mapAUC</code>	$\text{nx} \times \text{ny}$ matrix of impulse response function AUC values.
<code>mapAUCMRT</code>	$\text{nx} \times \text{ny}$ matrix of impulse response function $\frac{\text{AUC}}{\text{MRT}}$ values.
<code>mapIRF</code>	$\text{nx} \times \text{ny} \times \text{nt}$ matrix of voxel-wise impulse response functions.
<code>vectorTimesTrunc</code>	Truncated time vector for deconvolution algorithm.
<code>mapCCtransformed</code>	<code>mapCC</code> with pre-peak data removed; correct vein-artery lag.
<code>mapCCsmoothed</code>	<code>mapTumorTransformed</code> smoothed using <b>locfit</b> package.
<code>vectorAIFtrunc</code>	<code>vectorAIF</code> with pre-peak data removed.
<code>vectorAIFsmoothed</code>	<code>vectorAIF</code> smoothed using <b>locfit</b> package.
<code>CCmedianTransformed</code>	Median <code>mapCCtransformed</code> values over the region of interest.
<code>CCmedianSmoothed</code>	<code>CCmedianTransformed</code> smoothed using <b>locfit</b> package.
<code>IRFmedian</code>	Median impulse response function over the ROI.
<code>AUCmedian</code>	Median IRF AUC value over the ROI.
<code>AUCMRTmedian</code>	Median IRF $\frac{\text{AUC}}{\text{MRT}}$ value over the ROI.
<code>args</code>	Function arguments used for this run.
<code>plotParams</code>	$\text{nx}$ , $\text{ny}$ , $\text{nt}$ , ROI cropping coordinates, range of color scale.
<code>procTime</code>	Total time for analysis (minutes).
<code>DATversion</code>	Package version.

Table 3: Contents of summary file generated by the DAT function.

If we assume  $\vec{\text{IRF}}$  has a mono-exponential form, then errors in  $\text{AUC}_{T_f}$  and  $\text{MRT}_{T_f}$  calculations due to truncation, *i.e.*, neglecting the IRF from  $t = T_f$  to  $t = \infty$ , can be estimated by utilizing an estimated or nominal  $k_{ep}$  value for the tissue of interest. DAT implements the truncation error correction equations derived in Ferl *et al.* (2010) by calculating  $\text{AUC}_{T_f}/\text{AUC}_{\infty}$  and  $(\text{AUC}_{T_f} \cdot \text{MRT}_{\infty})/(\text{AUC}_{\infty} \cdot \text{MRT}_{T_f})$ . The truncation error correction factors are only rough approximations and should be interpreted with caution.

## 2.6. Voxel-wise numerical deconvolution

The code for performing numerical deconvolution on a voxel-wise basis, including calculation of the IRF and associated noncompartmental parameters, is executed by the DAT function. Most arguments for this function are assigned default values so that the function will process



a data file if the file name is specified (`file`) as an argument, along with the slice number of interest (`slice`) if the data file contains more than one slice. The remaining arguments may also be modified by the user and are described in the package documentation.

Also, voxels associated with apparent tissue concentrations greater than a fraction `maxC` of the maximum value of  $\vec{AIF}_s$  are excluded, effectively removing the majority of voxels associated with blood vessels. Each calculated  $\vec{IRF}$  vector containing a negative value whose absolute value is greater than 5% of the maximum positive value is removed from further analysis, as described in Ferl *et al.* (2010).

The primary output of the voxel-wise analysis script are parametric maps of  $\vec{IRF}$  (`mapIRF`),  $AUC_{T_f}$  (`mapAUC`) and  $AUC_{T_f}/MRT_{T_f}$  (`mapAUCMRT`); additional outputs are described in Table 3.

## 2.7. Whole-tumor numerical deconvolution

The `DAT` function also performs deconvolution analysis on median ROI data using the AIF vector shown in Figure 1 and the median contrast agent profile within the ROI (`vectorAIF` and `CCmedianSmoothed` from Table 3). The primary outputs of this function are the IRF and associated AUC and MRT, which are saved in the output file as `IRFmedian`, `AUCmedian` and `AUCMRTmedian`.

## 2.8. Advanced voxel diagnosis tool

Voxel-wise analyses of DCE-MRI scans utilize and generate large amounts of parameter estimates which may be summarized in the form of parametric maps. Although informative, key results are not always readily accessible when describing tissue heterogeneity in this manner. The `locator` function within R allows one to interact with an image by clicking on the display and returning the coordinates of the selected location as an R object. Specifically, tools provided in `DATforDCEMRI` display a single DCE-MRI slice in the main panel and plot the AIF, concentration-time data and any associated smoothed curves, all corresponding to the selected voxel. The calculated IRF is also displayed along with AUC and AUC/MRT values. The AVDT is automatically launched subsequent to successful completion of the deconvolution analysis; this option may be turned off by setting the argument `batch.mode = TRUE`. A previously generated DAT file may be visualized and explored using the AVDT by running the `DAT` function with the `file` as the sole argument; `DATforDCEMRI` will recognize the file as a DAT output file and automatically launch the AVDT.

# 3. A sample session

## 3.1. Loading the data

The first step is to load the data into R. In this example, the AIF and time vectors are saved in a single csv file that is read into the R session using the `read.csv` function. The contrast agent concentration and ROI arrays, which have been saved as MATLAB files in this example, are read into the session using the `readMat` function. This data is from a Phase II clinical trial of bevacizumab in adults with histologically proven grade III–IV glioma that was progressive or recurrent after radiation therapy (Vredenburgh *et al.* 2007); whole-ROI kinetic analysis of



the complete data set is described in Ferl *et al.* (2010) and Port *et al.* (2010).

```
R> csv <- read.csv("p0002_time_aif.csv")
R> voxel_data <- readMat("p0002_V6.mat")
R> TIMEvector <- csv$TIME
R> AIFvector <- csv$AIF
R> CCmap <- voxel_data$map[, , 1]$cc
R> ROImask <- voxel_data$mask[, , 1]$roi
```

### 3.2. Checking the data

The next step is to create a single data file to be processed by the `DAT` function. This is accomplished by running the function `DAT.checkData` and specifying the data vectors and arrays that were loaded in the previous section that correspond to the `vector.times`, `map.CC`, `mask.ROI` and `vector.AIF` arguments, as shown below. The variable `file.name` is the name that will be assigned to the newly generated file and `slice.stop` allows one to extract and save a range of data slices; here, the first nine of sixteen slices are extracted and saved for further analysis. The function `DAT.checkData` first checks that the dimensions of all arrays and vectors are consistent with one another, so that the vector-matrix operations can be preformed. If the data passes this check, it is saved in a single `RData` file.

```
R> DAT.checkData(file.name = "p0002", vector.times = TIMEvector,
+   map.CC = CCmap, mask.ROI = ROImask, vector.AIF = AIFvector,
+   slice.start = 1, slice.stop = 9)
```

checking dimensions of vectors and arrays...

```
length of vector.times is 65
length of vector.AIF is 65
dimensions of map.CC array are 256 x 256 x 9 slices x 65 time points
dimensions of mask.ROI array are 256 x 256 x 9 slices
```

...vector and array dimensions are okay.

Saving data in a single R file...

...file saved as p0002\_s1-s9.RData ...

...use the `DAT()` function to analyze data within this file.

The dimensions of all data arrays and vectors are printed on the R command line along with the name of the new file; the range of image slices is indicated in the file name.

### 3.3. Performing the deconvolution

The `DAT` function is used to perform deconvolution analysis on the data file generated by `DAT.checkData`. A minimum of two arguments are required for a multi-slice data file, the file name and the slice to be analyzed. In this example we've specified a third argument that tells `DAT` to save the deconvolution results in a `MATLAB` file format in addition to the `RData` file.

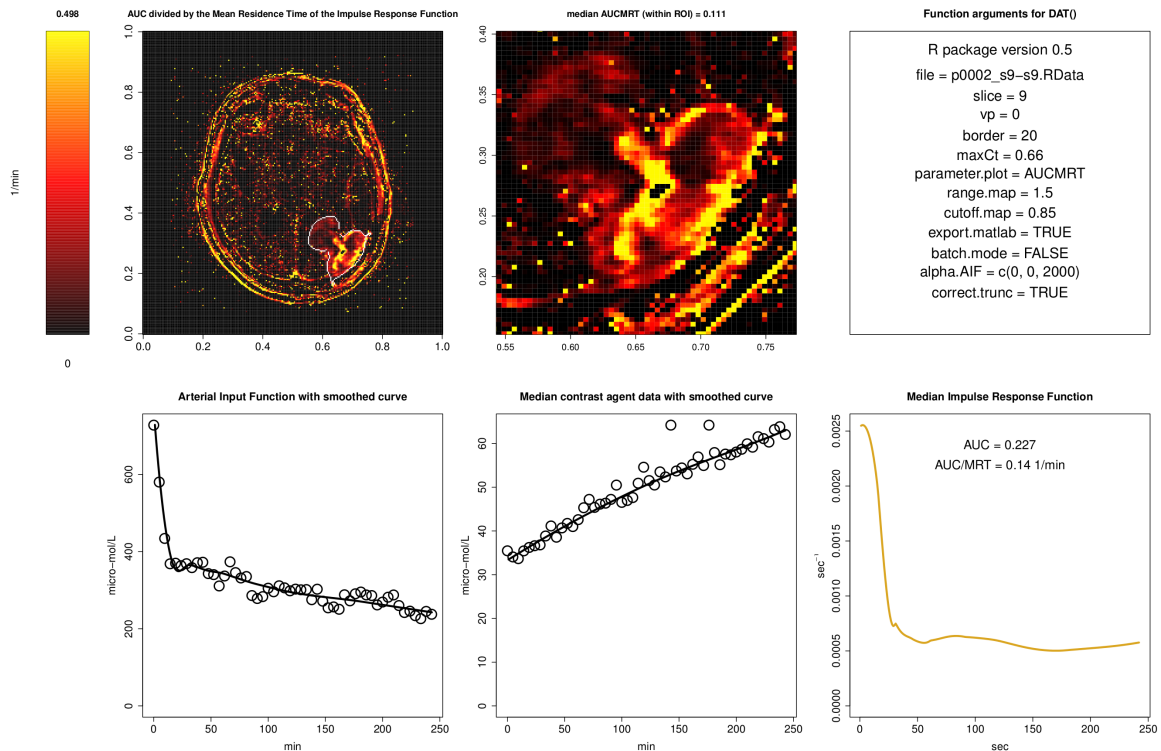


Figure 3: Image of a single axial slice from a clinical brain scan containing summary information associated with a single pre-treatment slice; produced by clicking the **Print to PDF** button within the main AVDT navigation window.

Once generated, the MATLAB file is not utilized by the **DATforDCEMRI** package but may be of use to those who wish to further process and/or visualize the data within MATLAB. By default, the RData results file is automatically loaded into R and the contents displayed using the AVDT. This feature may not be desirable when processing multiple slices in sequence and can be turned off via the `batch.mode` argument. The **Print to PDF** button will generate the PDF image shown in Figure 3 that contains summary information for that slice.

```
R> DAT(file = "p0002_s1-s9.RData", slice = 9, export.matlab = TRUE)
```

```
loading p0002_s1-s9.RData into R...
done in 0.14 minutes.
extracting and processing slice 9 for analysis...
done in 0.013 minutes.
performing deconvolution analysis on entire FOV...
..done in 12 minutes.
writing results to file...
..deconvolution results saved as DAT_p0002_s1-s9_s9_21Jun11-161651.RData
..deconvolution results saved as DAT_p0002_s1-s9_s9_21Jun11-161651.mat

loading DAT_p0002_s1-s9_s9_21Jun11-161651.RData into R...
```

```
done in 0.17 minutes.
---
point 1
x = 169
y = 76
AUC = 0.71 ; AUC/MRT = 0.493
---
point 2
x = 161
y = 62
AUC = 0.344 ; AUC/MRT = 0.192
---
point 3
x = 195
y = 102
AUC = 0.0724 ; AUC/MRT = 0.0338
---
---
session ended
---
```

Voxel coordinates, AUC and AUC/MRT values are printed on the R command line for each selected voxel while voxel specific data is plotted in the smaller panels.

## 4. Results

### 4.1. Whole-ROI analysis

The lower-left panels of Figures 3 and 4 display the AIF used for each scan along with the **locfit** smoothed curves, while the median contrast agent concentration curve across all voxels within the ROI is shown in the lower-middle panels, also with the associated smoothed curves. The ROI is outlined in white within the upper-left panels of Figures 3 and 4 with a magnified view of each ROI shown in the upper-middle panel. The image and AIF shown in Figure 1 correspond to those in Figure 3. The resulting IRF is plotted in the lower-right panels with the associated AUC and AUC/MRT values. Based on the median contrast agent concentration profile, AUC values for pre- and post-treatment scans are 0.227 and 0.145, while AUC/MRT values are 0.14 and 0.0887. The upper-right panels list the DAT function arguments used for that particular deconvolution analysis.

### 4.2. Voxel-wise analysis

Figures 3 and 4 display parametric maps of AUC/MRT values across the FOV for scans taken one day before and one day after administration of a single dose of bevacizumab. Malignant tumor tissue is clearly visible in the lower-right corner of the FOV image (upper-left panels) and the overall intensity of the lesion decreases subsequent to treatment. Across all voxels, median AUCs within the ROI are 0.212 and 0.144, before and after treatment, while median

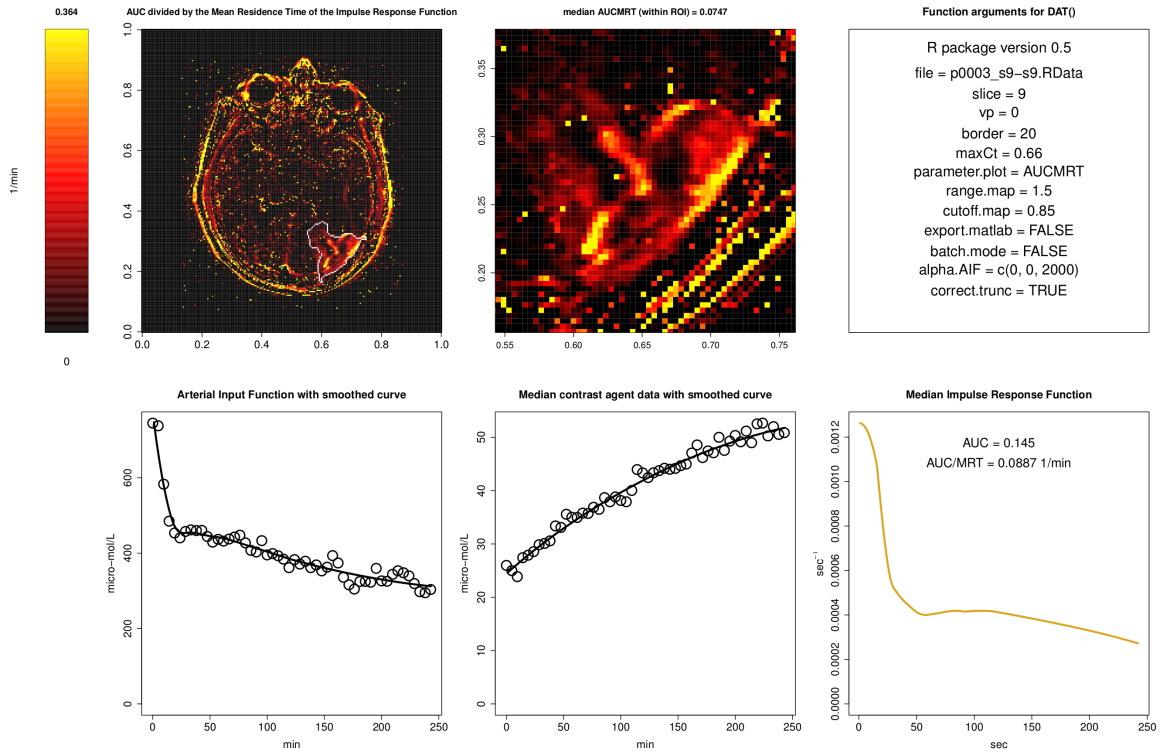


Figure 4: Image of a single axial slice from a clinical brain scan containing summary information associated with a single post-treatment slice; produced by clicking the **Print to PDF** button within the main AVDT navigation window.

AUC/MRT values are 0.111 and 0.0747 (Table 4). Note that these values differ slightly to those reported in Section 4.1, since we are comparing the median of voxel-wise fits to values calculated by fitting the model to the median contrast agent concentration curve. The parametric maps of tissue within the ROI (upper-middle panels) clearly illustrate the heterogeneous distribution of AUC/MRT values across the tumor.

### 4.3. Advanced voxel diagnosis tool

Figure 5 shows a screenshot of the advanced voxel diagnosis tool (AVDT) based on the simulated data set included in the **DATforDCEMRI** package. A parametric map of AUC/MRT values for the region of interest are displayed in the navigation window (upper-right panel) with maximum  $x$  and  $y$  values for the complete field of view scaled to one. The whole FOV window depicts an arbitrary ROI within a square field of simulated noise. The navigation window automatically zooms in on the ROI while, similar to Figures 3 and 4, the AIF and voxel-wise data are plotted in the smaller windows below. Selected voxels (green circles in the navigation window) are tracked on the R session command line on the right-hand side of the screen and the links within the navigation window allow one to print a summary image to a PDF file (Figures 3 and 4), display median contrast agent concentration and IRF curves and terminate the session.

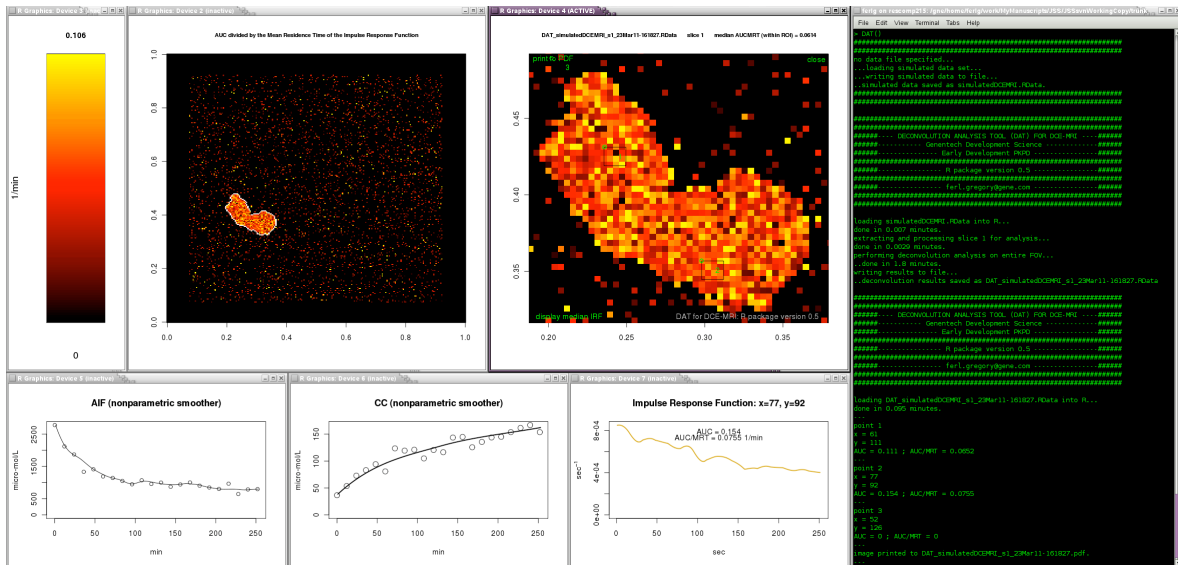


Figure 5: **DATforDCEMRI** screenshot based on the simulated data set, `DAT.simData`. A border of 20 voxels can be seen around the simulated noise field, specified by the `border` argument. The parametric maps display AUC/MRT values for each voxel, as specified by the `parameter.plot` argument. See the **DATforDCEMRI** manual for details on function arguments. The simulated data can be automatically analyzed and visualized by typing `demo(DAT, ask = FALSE)` at the R command prompt.

#### 4.4. Comparison to the Kety model

The Tofts version of the Kety model described in Equation 6 was applied to voxel-wise data within the ROIs drawn on the images shown in Figures 3 and 4, as described in Section 2.4, and compared to AUC and AUC/MRT values derived from deconvolution analysis of the same data. The left-hand panels of Figure 6 plot the AUC of the IRF on the ordinate and  $v_e$ , estimated by voxel-wise fitting of Equation 6 to the contrast agent concentration curves, on the abscissa. The right-hand panels of Figure 6 shows the same data after correction by the method described in section 2.5 and Ferl *et al.* (2010). The thin red line in each panel is calculated via linear regression ( $y = mx + b$ ) of the data and the thicker grey line is  $y = x$ . Median values are summarized in Table 4. These plots were also generated for voxel-wise AUC/MRT versus  $K^{\text{trans}}$  values and are qualitatively similar to those shown in Figure 6.

## 5. Discussion

We have described an R package that can be used to conduct deconvolution analysis of DCE-MRI data in an efficient and thorough manner. In this study, the entire field of view can be quickly analyzed, yielding a first approximation of the distribution of standard kinetic parameters from a single compartment model throughout the imaged tissue. Previous whole-ROI analysis Ferl *et al.* (2010) and the subsequent analysis described here (Figure 6, Table 4) show that kinetic parameters estimated using the methods employed by **DATforDCEMRI** are similar to  $K^{\text{trans}}$  and  $v_e$  parameters obtained by fitting the Tofts version of the Kety model to whole-ROI and voxel-wise data. Parametric maps generated by **DATforDCEMRI** may be

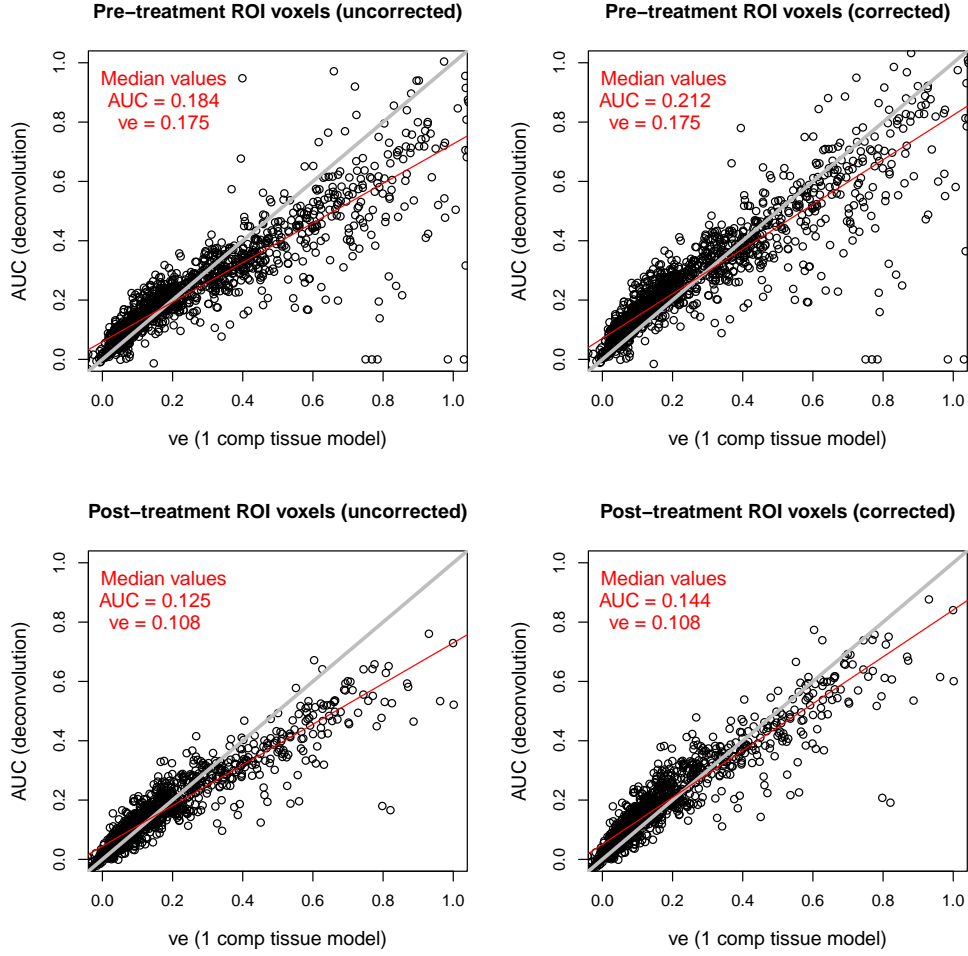


Figure 6: Voxel-wise AUC values compared to  $v_e$  values estimated by voxel-wise fitting of the Tofts version of the Kety model (Equation 6). Upper panels plot values based on scans taken one day before treatment; lower panels plot values based on scan taken one day after a single 10 mg/kg dose of bevacizumab. Right-hand panels show corrected values.

used to aid in the identification of ROIs and as a method to quickly assess the presence or absence of a treatment effect when comparing data from multiple scans.

Our AVDT allows one to easily visualize concentration-time data, as well as the associated smoothed curves, for selected voxels displayed on the parametric map. This device facilitates verification of computations that generate each value on the parametric map; one can quickly verify that the smoother and deconvolution operations performed properly for voxels of interest as well as view voxel-specific data related to regions of heterogeneous uptake throughout the image.

Independence from model structure is a key feature of the numerical deconvolution method, allowing one to perform kinetic analysis on DCE-MRI data without going through the process

	Pre-treatment	Post-treatment	% change
AUC	0.184/0.212	0.125/0.144	-32
$v_e$	0.175	0.108	-38
AUC/MRT	0.14/0.111	0.0938/0.0747	-33
$K^{\text{trans}}$	0.0918	0.0592	-36

Table 4: Median voxel-wise IRF AUC and AUC/MRT (uncorrected/corrected) values compared to median voxel-wise  $v_e$  and  $K^{\text{trans}}$  values for data under consideration here (Figures 3 and 4). The right-hand column indicated the percentage change in values between post- and pre-treatment. Whole-ROI kinetic analysis of the complete data set is described in Ferl *et al.* (2010) and Port *et al.* (2010).

of determining the “best” model structure. Although the scope of this paper is limited to analysis of brain acquisitions, our deconvolution approach is quite robust and may be applied to any type of DCE-MRI data and, indeed, any type of input/output data collected over a time course. We have previously analyzed data from breast and liver lesions using this software.

The computational simplicity of numerical deconvolution is also a potential advantage. Parameter estimation is an iterative process that requires a system of equations to be solved for each step taken while navigating the surface of the objective function in the search for a minimum value. Analytical solutions to the Kety model may be fitted to DCE-MRI data (Whitcher and Schmid 2011a,b), significantly reducing the complexity of this operation by eliminating the need for an ODE solver; however, this requires a functional form to be assumed for the AIF. Numerical deconvolution is a non-iterative algebraic procedure that makes few assumptions and, due to its computational simplicity, can be performed in alternative GPU-based high-speed programming environments (Ng 2011).

The utility of these functions is twofold: (1) Quickly analyze all imaged tissue within the field of view and identify potential regions of interest, (2) quickly assess the presence or absence of a treatment effect when comparing scans of a single patient obtained before and after treatment; the study described here (voxel-wise analysis) and Ferl *et al.* (2010) (whole-ROI analysis) show that percent changes of AUC and AUC/MRT values between scans were similar to changes in  $K^{\text{trans}}$  and  $v_e$  values obtained by fitting the Tofts version of the Kety model to the contrast agent data.

## Acknowledgments

Ruediger E. Port, M.D. (Genentech) for his guidance, support and critical review of this manuscript and Daniel P. Barboriak, M.D. (Duke University Medical Center) for providing clinical DCE-MRI data. Michel Friesenhahn, Ph.D. (Genentech) and Lisa J. Bernstein, Ph.D. (Genentech) for statistical support and Lu Xu, Ph.D. (Genentech) for image processing support. Frank-Peter Theil, Ph.D. and Paul J. Fielder, Ph.D. for continued support of this work within Early Development PKPD at Genentech. Michael Lawrence, Ph.D. (Genentech) for advice on R package creation.



## References

- Bengtsson H (2011). *R.utils: Various Programming Utilities*. R package version 1.8.2, URL <http://CRAN.R-project.org/package=R.utils>.
- Choyke PL, Dwyer AJ, Knopp MV (2003). “Functional Tumor Imaging with Dynamic Contrast-Enhanced Magnetic Resonance Imaging.” *Journal of Magnetic Resonance Imaging*, **17**(5), 509–520.
- Evans WR (1954). *Control-System Dynamics*. McGraw-Hill, New York.
- Fan X, Karczmar GS (2009). “A New Approach to Analysis of the Impulse Response Function (IRF) in Dynamic Contrast-Enhanced MRI (DCEMRI): A Simulation Study.” *Magnetic Resonance in Medicine*, **62**(1), 229–39.
- Ferl GZ (2011). *DATforDCEMRI: Deconvolution Analysis Tool for Dynamic Contrast-Enhanced MRI*. R package version 0.5, URL <http://CRAN.R-project.org/package=DATforDCEMRI>.
- Ferl GZ, Xu L, Friesenhahn M, Bernstein LJ, Barboriak DP, Port RE (2010). “An Automated Method for Nonparametric Kinetic Analysis of Clinical DCE-MRI Data: Application to Glioblastoma Treated With Bevacizumab.” *Magnetic Resonance in Medicine*, **63**(5), 1366–75.
- Kety SS (1951). “The Theory and Applications of the Exchange of Inert Gas at the Lungs and Tissues.” *Pharmacological Reviews*, **3**(1), 1–41.
- Knuth DE (1984). “Literate Programming.” *The Computer Journal*, **27**(2), 97–111.
- Leisch F (2002). “Dynamic Generation of Statistical Reports Using Literate Data Analysis.” In W Härdle, B Rönz (eds.), *COMPSTAT 2002 – Proceedings in Computational Statistics*, pp. 575–580. Physica-Verlag, Heidelberg.
- Loader C (1999). *Local Regression and Likelihood*. Springer-Verlag, New York.
- Loader C (2010). *locfit: Local Regression, Likelihood and Density Estimation*. R package version 1.5-6, URL <http://CRAN.R-project.org/package=locfit>.
- Ng C (2011). “Novel GPU-Based Parallelized Quasi-Random Parametric Expectation-Maximization (QRPEM) Estimation Method for Population Data Analysis.” In *Abstracts of the Annual Meeting of the Population Approach Group in Europe*. Athens, Greece. ISSN 1871–6032. URL <http://www.page-meeting.org/?abstract=2051>.
- O’Connor JP, Jackson A, Parker GJ, Jayson GC (2007). “DCE-MRI Biomarkers in the Clinical Evaluation of Antiangiogenic and Vascular Disrupting Agents.” *British Journal of Cancer*, **96**(2), 189–195.
- Padhani AR (2002). “Dynamic Contrast-Enhanced MRI in Clinical Oncology: Current Status and Future Directions.” *Journal of Magnetic Resonance Imaging*, **16**(4), 407–422.

- Port RE, Bernstein LJ, Barboriak DP, Xu L, Roberts TP, van Bruggen N (2010). “Non-compartmental Kinetic Analysis of DCE-MRI Data from Malignant Tumors: Application to Glioblastoma Treated with Bevacizumab.” *Magnetic Resonance in Medicine*, **64**(2), 408–417.
- R Development Core Team (2011). *R: A Language and Environment for Statistical Computing*. R Foundation for Statistical Computing, Vienna, Austria. ISBN 3-900051-07-0, URL <http://www.R-project.org/>.
- Rescigno A, Segre G (1966). *Drug and Tracer Kinetics*. Blaisdell Publishing Company, Waltham, Massachusetts. Translated from Italian by Piero Ariotti.
- Schmid VJ, Whitcher B, Padhani AR, Yang GZ (2009). “Quantitative Analysis of Dynamic Contrast-Enhanced MR Images Based on Bayesian P-Splines.” *IEEE Transactions in Medical Imaging*, **28**(6), 789–798.
- Tofts PS (1997). “Modeling Tracer Kinetics in Dynamic Gd-DTPA MR Imaging.” *Journal of Magnetic Resonance Imaging*, **7**(1), 91–101.
- Tofts PS, Brix G, Buckley DL, Evelhoch JL, Henderson E, Knopp MV, Henrik BW, Larsson MD, Lee TY, Mayr NA, Parker GJM, Port RE, Taylor J, Weisskoff RM (1999). “Estimating Kinetic Parameters from Dynamic Contrast-Enhanced T1-Weighted MRI of a Diffusable Tracer: Standardized Quantities and Symbols.” *Journal of Magnetic Resonance Imaging*, **10**(3), 223–232.
- Tofts PS, Kermode AG (1991). “Measurement of the Blood-Brain Barrier Permeability and Leakage Space Using Dynamic MR Imaging. 1. Fundamental Concepts.” *Magnetic Resonance in Medicine*, **17**(2), 357–67.
- Vredenburgh JJ, Desjardins A, Herndon JEn, Dowell JM, Reardon DA, Quinn JA, Rich JN, Sathornsumetee S, Gururangan S, Wagner M, Bigner DD, Friedman AH, Friedman HS (2007). “Phase II Trial of Bevacizumab and Irinotecan in Recurrent Malignant Glioma.” *Clinical Cancer Research*, **13**(4), 1253–1259.
- Whitcher B (2010). “CRAN Task View: Medical Image Analysis.” Version 2010-11-30, URL <http://CRAN.R-project.org/view=MedicalImaging>.
- Whitcher B, Schmid VJ (2011a). *dcemriS4: A Package for Medical Image Analysis (S4 Implementation)*. R package version 0.43, URL <http://CRAN.R-project.org/package=dcemriS4>.
- Whitcher B, Schmid VJ (2011b). “Quantitative Analysis of Dynamic Contrast-Enhanced and Diffusion-Weighted Magnetic Resonance Imaging for Oncology in R.” *Journal of Statistical Software*, **44**(5), 1–29. URL <http://www.jstatsoft.org/v44/i05/>.
- Zeileis A (2005). “CRAN Task Views.” *R News*, **5**(1), 39–40. URL <http://CRAN.R-project.org/doc/Rnews/>.

**Affiliation:**

Gregory Z. Ferl  
Genentech, Inc.  
Development Sciences  
1 DNA Way, Mail stop 463A  
South San Francisco, CA, United States of America  
E-mail: [ferlg@gene.com](mailto:ferlg@gene.com)